Substrata Mechanical Stiffness Can Regulate Adhesion of Viable Bacteria

Jenny A. Lichter,[†,‡] M. Todd Thompson,[‡,§] Maricela Delgadillo,[†] Takehiro Nishikawa,[†,||] Michael F. Rubner,[†] and Krystyn J. Van Vliet*[,†]

Department of Materials Science and Engineering, Massachusetts Institute of Technology, Cambridge, Massachusetts 02139, Harvard-MIT Division of Health Sciences and Technology, Massachusetts Institute of Technology, Cambridge, Massachusetts 02139

Received December 31, 2007; Revised Manuscript Received March 7, 2008

The competing mechanisms that regulate adhesion of bacteria to surfaces and subsequent biofilm formation remain unclear, though nearly all studies have focused on the role of physical and chemical properties of the material surface. Given the large monetary and health costs of medical-device colonization and hospital-acquired infections due to bacteria, there is considerable interest in better understanding of material properties that can limit bacterial adhesion and viability. Here we employ weak polyelectrolyte multilayer (PEM) thin films comprised of poly(allylamine) hydrochloride (PAH) and poly(acrylic acid) (PAA), assembled over a range of conditions, to explore the physicochemical and mechanical characteristics of material surfaces controlling adhesion of *Staphylococcus epidermidis* bacteria and subsequent colony growth. Although it is increasingly appreciated that eukaryotic cells possess subcellular structures and biomolecular pathways to sense and respond to local chemomechanical environments, much less is known about mechanoselective adhesion of prokaryotes such as these bacteria. We find that adhesion of viable *S. epidermidis* correlates positively with the stiffness of these polymeric substrata, independently of the roughness, interaction energy, and charge density of these materials. Quantitatively similar trends observed for wild-type and actin analogue mutant *Escherichia coli* suggest that these results are not confined to only specific bacterial strains, shapes, or cell envelope types. These results indicate the plausibility of mechanoselective adhesion mechanisms in prokaryotes and suggest that mechanical stiffness of substrata materials represents an additional parameter that can regulate adhesion of and subsequent colonization by viable bacteria.

1. Introduction

The design of functional materials to control the formation of biofilms, structured communities of bacteria protected by a polysaccharide matrix, has been the subject of numerous research efforts. Hospital-acquired infections represent an estimated $4.5 billion cost,[1] with an associated annual mortality of 100000 persons in the U.S. alone.[2] The commensal bacterial species *Staphylococcus epidermidis* is the most common agent of infection,[1,3] exceeding the infection rate of methicillin-resistant *Staphylococcus aureus* (MRSA), with virulence often attributed to initial attachment of a viable bacterial population to the surface[4] of a medical device and subsequent formation of a mature biofilm.

Current approaches to limit bacterial colonization have focused on chemical degradation of stably adhered bacteria, including surface functionalization with microbicidal agents,[5–7] surface impregnation with slow-releasing biocides such as gold or silver[8–11] and antibiotics,[5,12] or surface functionalization of specific antimicrobial peptides and polymers.[7,13–15] Because biofilm formation requires the initial, stable attachment of a viable bacteria population on a surface,[4] another promising approach to limiting microbial colonization is prevention of bacterial adhesion to material substrata prior to colonization. Others have reported that poly(ethylene glycol)-conjugated polypeptides confer adhesion resistance and suggested that such results may be due to high degrees of substrata surface hydration;[16] this speculation was not systematically tested. More generally, the development of a versatile and comprehensive approach to reduce stable bacterial adhesion to surfaces has been limited by incomplete understanding of the regulating physicochemical material properties. Physical characteristics such as surface roughness do not appear to impact bacterial adhesion consistently, with some studies reporting reduced adhesion of *S. epidermidis* to smoother surfaces[17] and others finding no conclusive correlation.[1,17–21] Material surface charge and hydrophobicity have been reported to be crucial during the primary, kinetic step of adhesion.[22–25] However, several studies have reported no correlation between microbial adhesion and substratum hydrophobicity measured via contact angle measurements[18,19] and claimed the presentation of surface functional groups capable of charge transfer (Lewis acid/base character of the surface) as the critical surface factor governing bacterial adhesion.[26–28] As the specific interactions among bacteria, solvents, and substrata can each contribute independently to the efficiency of adhesion, others have claimed the dominant factor to be total interaction energy between the microbe, liquid media, and substrata material, usually expressed as the work of adhesion.[28–30] Beyond the potential strain-dependence and the convolution of competing factors such as surface roughness and

* To whom correspondence should be addressed. Address: MIT Room 8-237,77 Massachusetts Avenue, Cambridge, MA 02139. Tel.: 617-253-3315. Fax: 617-253-8745. E-mail:krystyn@mit.edu.

[†] Department of Materials Science and Engineering, Massachusetts Institute of Technology.

[‡] Authors contributed equally.

[§] Harvard-MIT Division of Health Sciences and Technology, Massachusetts Institute of Technology.

[||] Current affiliation: National Cardiovascular Center, Advanced Medical Engineering Center, 5-7-1 Fujishirodai, Suita, Osaka 575-0873 Japan.

10.1021/bm701430y CCC: $40.75
Published on Web 05/02/2008

surface energy in the synthetic surfaces considered, such contradictory results may indicate unrecognized surface properties that modulate bacterial attachment. Here, we engineer material surfaces of quantified surface roughness, charge density, interaction energy, and elastic moduli to consider whether the mechanical compliance of the surface, now widely appreciated to modulate the adhesion and function of eukaryotic cells,[31–35] may also regulate bacterial adhesion to underlying substrata. *S. epidermidis*, a spherical Gram positive (G+) microbe, was the predominant bacterium type in our study. This microbe serves as an established model for bacterial attachment,[36] as well as a common cause of medical-device related and hospital-acquired infections.[1,3,37] Strategies for prevention of initial colonization and infection with *S. epidermidis* are clinically important, as these strains are increasingly resistant to antibiotics.[38] *E. coli*, a rod-shaped Gram negative (G−) microbe, and its actin analogue mutant form Δ*mreB E. coli* were also tested to consider whether our observations were limited to only specific strains, cell shapes, or Gram-stain classes.

To vary the physicochemical and mechanical properties of the substrata, we employed a class of synthetic polymer thin films termed weak polyelectrolyte multilayers (PEMs) comprising the polyelectrolytes, poly(allylamine) hydrochloride (PAH), and poly(acrylic acid) (PAA). The chemical functionality and mechanical compliance of such films can be adjusted by simple variations of the layer-by-layer assembly conditions, such as choice of polyanion/polycation or assembly pH,[33] and can be applied to a wide range of surfaces requiring biofilm prevention, including polymers, glasses,[39] and metals.[13] The effective elastic modulus E or stiffness of such hydrated films under in vitro culture conditions can be varied over several orders of magnitude by manipulation of assembly pH.[33] We and others have shown that this substrata stiffness modulates tissue cell adhesion independently of physicochemical characteristics, such as adhesive ligand density.[31,32,40,41] Through extensive characterization of these tunable polymeric substrata, we demonstrate that *S. epidermidis* exhibits mechanoselective adhesion. As a result, bacterial colonization can be significantly reduced by modulating the compliance of the material substrata, independently of short and long-range physicochemical properties of the cell-material interface.

2. Experimental Section

2.1. PEM Assembly. Polyelectrolyte multilayers were assembled as previously described, in a layer by layer (LbL) automated assembly of alternate dipping into polycation/anion solutions.[42] Solutions at 10^{-2} M in 18 MΩ Milli-Q water of PAA (poly(acrylic acid); $M_w \geq 200000$ g/mol; 25% aqueous solution; Polysciences (previously labeled as $M_w = 90000$ g/mol)) or PAH (poly(allylamine hydrochloride); $M_w = 70000$ g/mol; Polysciences) were pH-adjusted using 1 M HCl and NaOH. Multilayers were assembled PAA first on aminoalkylsilane coated glass (Sigma-Aldrich) or, for Figure 1 only, on medical grade titanium (ASTM F67, President Titanium, Hanson, MA). Notation refers to the assembly conditions with the PAA pH followed by the PAH pH, that is, a 3.5/8.6 PEM was assembled using PAA at pH 3.5 and PAH at pH 8.6. All PEMs were prepared to dry thicknesses of ~50 nm, which required variation in the total number of layering (dipping) cycles at each assembly pH. The samples included 2.0/2.0 (9.5 bilayers), 4.0/4.0 (7.5 bilayers), 6.5/6.5 (49.5 bilayers), 3.5/7.5 (5.5 bilayers), and 3.5/8.6 (5.5 bilayers). The following samples studied the effect of masking an underlying PEM substrata in Figure 4: 6.5/6.5 (50 bilayers; PAH final dip) plus 0.5 bilayer of pH 2.0 PAA; 6.5/6.5 (49.5 bilayers) plus one bilayer of 2.0/2.0; and 2.0/2.0 (9.5 bilayers) plus pH 6.5 PAH. The propensity for assembly pH-modulated extent of ionic crosslinking in these weak PEMs differs significantly from strong PEMs used by others in studies for aspirated deadhesion of eukaryotic cells.[43]

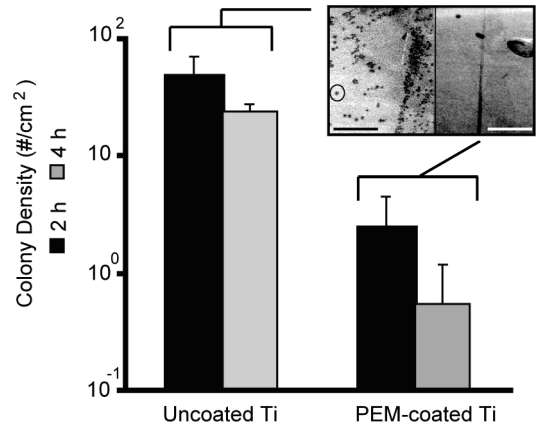

Figure 1. PEMs reduce bacterial adhesion on medical grade titanium. Adhesion of waterborne *S. epidermidis* is reduced by coating with a pH-tunable polyelectrolyte multilayer (PEM) film of PAA and PAH assembled at pH 2.0 and is stable at both 2 h (inset; circle indicates one such colony) and 4 h incubation duration. Scale bars = 5 mm.

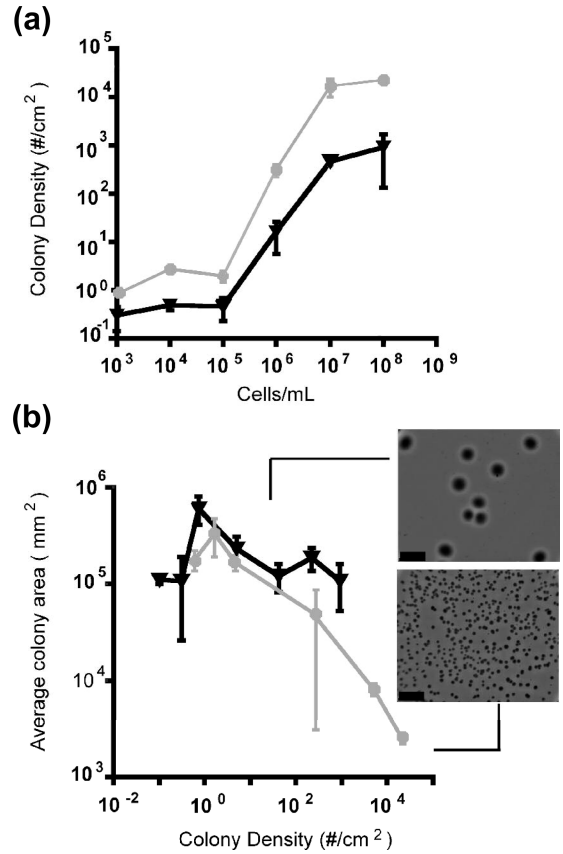

Figure 2. Bacterial colonies observed for 10^3–10^8 *S. epidermidis*/mL in 150 mM NaCl PBS. (a) Average colony number per unit substrata area increased with increasing incubation concentration for greater than 10^5 cells/mL; for all concentrations, the density of colonies observed on the PEM substrata assembled at pH 6.5 (●) was significantly greater than that observed on the substrata assembled at pH 2.0 (▼). (b) For the given initial concentration, colony number was greater and colony size was smaller on stiffer substrata, supporting a model whereby bacteria attachment is modulated in part by substrata stiffness, but subsequent growth is affected predominantly by available space and nutrients. Scalebars = 500 μm.

2.2. PEM Elastic Moduli. The effective elastic moduli of these substrata E, as determined from nanoindentation force-displacement responses acquired from an atomic force microscope (3D Molecular

Force Probe, Asylum Research, Santa Barbara, CA), were quantified as previously described.[33] Silicon nitride cantilevers (MLCT-AUHW, Veeco Metrology Group, Sunnyvale, CA) were used to indent PEMs to maximum depths of <20 nm, with a threshold filter to maintain equal loads for each indentation. The probe radius of curvature R_p was ~50 nm; cantilever spring constant k was nominally 0.1 N/m and was experimentally determined for each cantilever.[44] Nanoindentation was performed in an acoustic isolation enclosure (Herzan, Inc.) at room temperature in 0.2 μm, filtered PBS or Milli-Q water. Nanoindentation force-depth data were analyzed in IGOR (Wavemetrics, Lake Oswego, OR) and E was determined according to a modified Hertzian contact model;[33] see Supporting Information.

2.3. Substrata Surface Energy and Interaction Energy. To determine the total interaction energy and surface tension components of the substrata, liquid contact angles were measured for the polar solvents water and ethylene glycol and the apolar solvents hexadecane and diiodomethane. A total of 5−10 measurements were performed on each sample using the sessile drop technique, and contact angles were recorded for static, advancing, and receding drops. Contact angles were measured using a camera-equipped Advanced Surface Systems machine. Liquid contact angles were used to determine thermodynamic properties of the surface−bacterial cell−liquid interface according to the Lewis acid−Lewis base theory of Van Oss.[28] Using the Van Oss approach, liquid contact angles of three or more test solvents are measured and then the nonlinear Van Oss−Young equations solved simultaneously; see Supporting Information.

2.4. Substrata Surface Charge Density. Surface charge density Q was analyzed for PEMs 2.0/2.0 and 6.5/6.5 via AFM force spectroscopy (3DMFP, Asylum Research), using cantilevered carboxylic acid-functionalized polystyrene spheres of approximately 3 μm radius (BioForce Nanosciences, Ames, IA; nominal $k \sim 0.1$ N/m). Force−distance curves were first acquired in deionized water using a test surface comprised of mercaptoundecanoic acid (MUA)-functionalized gold with calibrated Q[45,46] of $Q = -18$ mC/m^2, from which the Q of the colloidal probe was calculated using models adapted from Rixman et al.; [45,46] see Supporting Information. We deemed this approach to be a more direct and representative measurement of surface charge density apparent to an approaching microscale microbe, relative to alternative characterizations such as streaming and standard Zeta potential measurements, the latter of which requires a degree of antiflocculation unattainable for several of the PEMs considered.

2.5. Bacterial Attachment Assays. Waterborne bacterial attachment assays were adapted from the established protocol of Tiller et al.[7] Briefly, Miller Luria−Bertani or LB-Miller broth (purchased from VWR) was inoculated with a monoclonal strain of *Staphylococcus epidermidis* (*S. epidermidis*, ATCC #14990), *E. coli* (w3100 strain of well-documented lineage ATTC #14948),[47] or *E. coli* mutant strain Δ*mreB*, using a sterile loop and incubated overnight at 37 C while shaking. Two 50 mL aliquots of culture were centrifuged at 2700 RPM (RCF 1010 g) for 10 min at 4 C (see ref 7), the LB-Miller broth decanted, and the bacterial cell pellets resuspended in 150 mM NaCl PBS, the molarity of 1× PBS (VWR). Following resuspension, the cells were centrifuged twice (5 min, 2700 RPM) to ensure complete removal of LB broth, with a final resuspension in 18 MΩ Millipore water. The resuspension was serially diluted with water from 10^9 cells/mL (measured via optical density) to create suspensions of 10^3−10^8 cells/mL. Studies in water were conducted at 10^7 cells/mL for *S. epidermidis* and 0.5×10^7 cells/mL for *E. coli* due to overall higher adhesion efficiency of *E. coli*. Samples (in triplicate for each condition) were placed in the bacterial solutions for 2 h at room temperature followed by agitation in three water bath rinses, each for ~5 s. Samples were incubated under 1% LB agar (VWR) gel overnight, and colonies were counted to determine the ability of viable bacteria to attach to each sample. Initial adhesion assays in PBS (Figure 2) were identical to those in water, except that final resuspensions occurred in PBS and incubation periods occurred at 37 C with shaking; note that the salt titration assay of Figure 5 was conducted at room temperature without agitation. Samples with few colonies were hand counted. For densely populated slides, at least 10 digital images per sample were acquired with a 4× objective using an inverted optical microscope (Leica), and semiautomated image analysis was conducted; see Supporting Information. Statistical analysis was conducted using the Tukey−Kramer multiple-comparisons post-test analysis of variance (ANOVA).

3. Results and Discussion

3.1. Bacterial Colonization can be Reduced by Material Substrata Modifications. Although the competing mechanisms remain unclear, a large body of data suggests that both physical and chemical modifications of a material surface can be engineered to limit bacterial colonization.[5–10,12,13,20,22] For example, as shown in Figure 1, coating surgical-grade titanium alloy with a synthetic PEM of PAA and PAH reduced colony density of waterborne *S. epidermidis* bacteria by orders of magnitude after immersion in 10^7 bacteria/mL. Reduced colonization over both 2 and 4 h incubation timescales is relevant to medical procedure durations involving, for example, cardiac assist and orthopedic implant devices.[48] This PEM was ionically crosslinked through layer-by-layer dipping of the titanium into polycation and polyanion solutions at pH 2.0 (see Experimental Section) prior to full hydration and equilibration in sterile, deionized, distilled water.

3.2. Weak Polyelectrolyte Multilayers Modulate Stable Adhesion of *S. epidermidis* Bacteria. We varied the assembly pH of the PEM substrata to consider how such modifications might affect *S. epidermidis* colonization of these surfaces. Assembly of these weak PEMs at pH 2.0 results in a substrata of much lower stiffness (effective elastic modulus $E \sim 1$ MPa) than at pH 6.5 ($E \sim 100$ MPa).[33] As shown in Figure 2a, for a 2 h incubation of substrata in seeding concentrations ranging from 10^3 to 10^8 bacteria/mL of 150 mM NaCl phosphate-buffered saline, average colony density (number of colonies per unit substrata) was greater on mechanically stiffer substrata. For a given seeding concentration, the average colony size observed after 24 h culture was also much greater on the more compliant substrata; this suggested that the properties of these substrata possibly affected both bacterial adhesion and colony growth. Figure 2b suggests that the observed differences in colony density occurred at the stable adhesion step: colony size depended on colony density for both substrata. In other words, the initial bacterial attachment increased with increasing substrata stiffness, but the subsequent colony growth was likely limited by available space and nutrients postadhesion.

3.3. Characterization of Polymeric Substrata Properties. To consider the characteristics of the polymer substrata that directly affect attachment of *S. epidermidis*, we conducted a larger study in deionized water to eliminate possible charge shielding and reorganization of the ionic crosslinks within the PEM substrata in salt solutions. For the substrata considered, we quantified the mechanical compliance and the physicochemical surface properties considered to affect microbial adhesion. Table 1 indicates physicochemical and mechanical characteristics of substrata employed in the larger study. PAA and PAH were adjusted to the same pH (e.g., PAA/PAH 2.0/2.0) as well as to different pH (e.g., PAA/PAH 3.5/7.5) during assembly to increase the range of substrata properties. Atomic force microscopy (AFM) imaging of hydrated substrata in tapping mode indicated a range of root-mean-square (rms) surface roughness from 3 to 30 nm. AFM-enabled nanoindentation of the PEMs hydrated in deionized water indicated an average elastic modulus E ranging over 2 orders of magnitude from the stiffest PEMs assembled at pH 6.5 ($E = 80.4$ MPa) to the most compliant

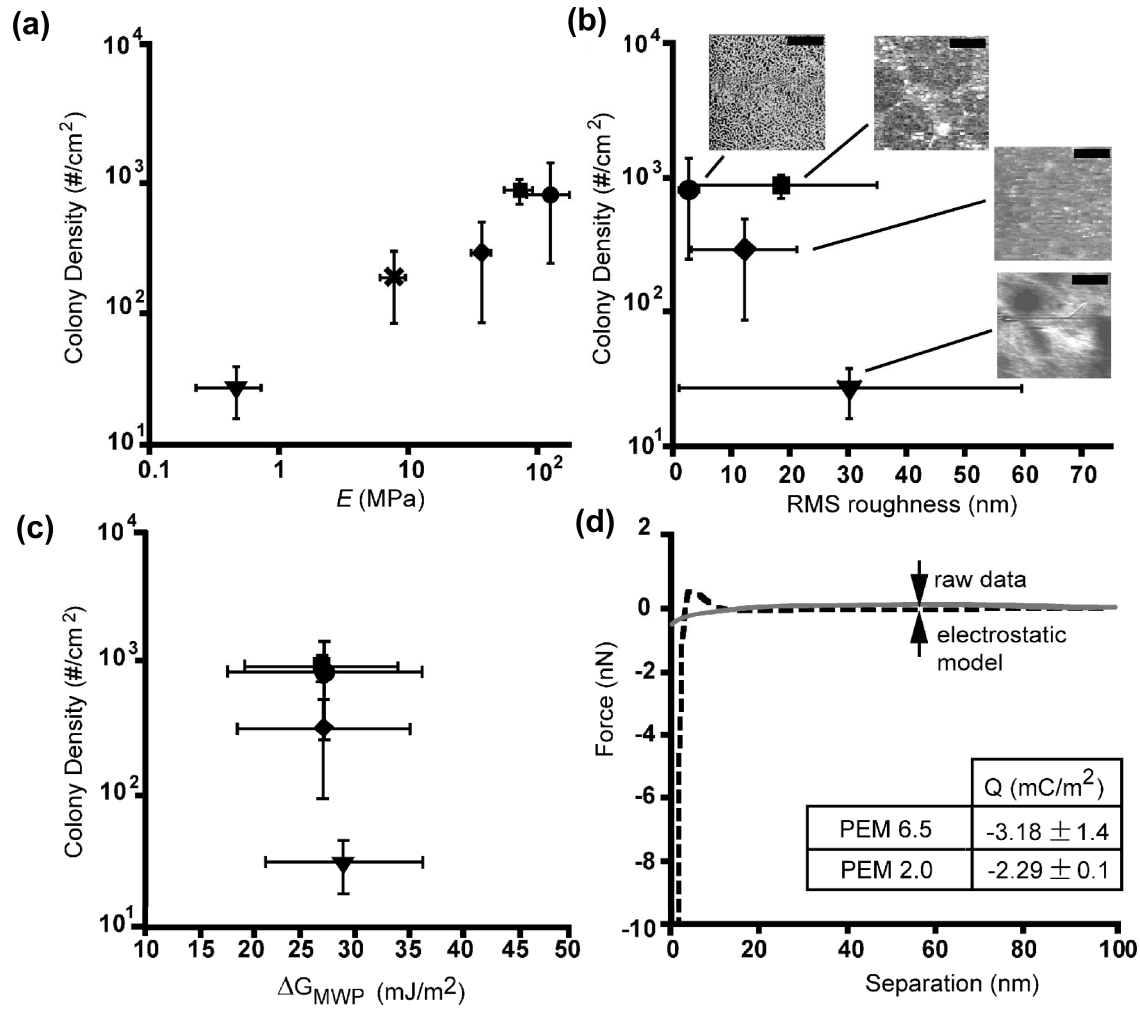

Figure 3. *S. epidermidis* colony density as a function of various surface parameters. (a) Colony density varies directly with substrata elastic moduli E. All sample differences statistically significant (1-way ANOVA, $a = 0.05$, $P = 0.0059$). (b) Colony density is independent of rms surface roughness of the substrata. Scale bar = 5 μm. (c) Total interaction energy ΔG_{MWP} for the microbe−water−PEM system is statistically indistinguishable among all substrata considered (1-way ANOVA, $a = 0.05$, $P = 0.987$). (d) Surface charge density Q, as measured via electrostatic repulsion of a carboxylated spherical probe in Milli-Q water (see Experimental Section), is within standard deviation for PEMs assembled at pH 2.0 (compliant) and pH 6.5 (stiff). Representative charge repulsion curve (solid) and constant-surface-charge model fit (dashed) are shown. Symbols refer to the following PEMs: PAA/PAH 2.0/2.0 (▼), 4.0/4.0 (**x**) in (a) to consider intermediate substrata stiffness, 6.5/6.5 (●), 3.5/7.5 (■), and 3.5/8.6 (♦).

PEMs assembled at pH 2.0 ($E = 0.8$ MPa), consistent with our previously reported mechanical characterization of these PEMs in 150 mM NaCl phosphate buffered saline (1× PBS).[33]

Surface energies of interaction were calculated according to Van Oss' adaptation of Young's theory,[28] which correlates the interfacial tension and surface energy of interaction between materials in a solvent. Four solvents of disparate surface tension and polarity were used (see Experimental Section). The apolar and polar components of this surface tension relate to the Lifshitz−van der Waals and Lewis acid−Lewis base (charge transfer) character of each sample, respectively; both interactions are thought to influence bacterial adhesion.[28] Thermodynamic properties at the PEM−liquid interface have been characterized using the Van Oss approach to describe the assembly process but, to our knowledge, have not been applied in the context of microbe−water−PEM (MWP) interactions.[49] The surface interaction energies ΔG_{MWP} for all PEM substrata considered narrowly ranged from 26−29 mJ/m^2 and were statistically indistinguishable (see Supporting Information for the component determinants of ΔG_{MWP}).

To assess net surface charge density Q present at the fluid−PEM interfaces, the substrata assembled at pH extremes of 2.0 and 6.5 were probed in deionized water using a carboxylated colloidal sphere approximately the size of a few bacteria (3 μm radius; see Experimental Section). As PEM assembly relies on charge overcompensation to increase substrata thickness, one might expect the observed net-negative Q because the anionic polymer, PAA, was layered last. However, it is important to note that although these polymeric substrata are termed multilayers due to the layer-by-layer assembly process, the structure is not striated and the polyanion and polycation macromolecular chains are highly entangled. Charge densities of PEMs assembled at pH 2.0 and 6.5 were well within one standard deviation ($Q = -2.29 \pm 0.1$ mC/m^2 and -3.18 ± 1.4 mC/m^2, respectively); see Figure 3d. Q was unchanged in solutions of higher ionic strength, such as 150 mM NaCl PBS, although charge is effectively screened in such ionic solutions.

In summary, the nominal elastic moduli of these substrata varied over approximately 2 orders of magnitude, while the other physicochemical characteristics considered to regulate bacterial adhesion varied to a known or statistically indistinguishable extent. We confirmed that these surface properties were

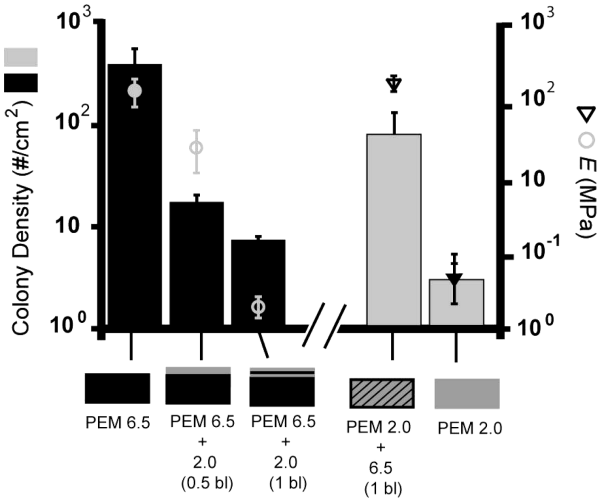

Figure 4. Multilayer addition to modulate composite substrata stiffness. Addition of 0.5 and 1 bilayer of PAA/PAH at pH 2.0 onto a stiff PEM (pH 6.5) decreases the effective mechanical stiffness of the substrata (gray circles) and decreases the bacterial colony density (black columns). Addition of one bilayer of PAA/PAH at pH 6.5 to a compliant PEM (pH 2.0) increases effective stiffness (black triangles) and bacterial colony density (gray columns). We observed statistically significant differences in the colony densities among the masked PEM 6.5 substrata and among the masked PEM 2.0 substrata, respectively (1-way ANOVA, $a = 0.05$ with $P = 0.00027$ and 0.0031, respectively).

unchanged when the substrata were hydrated over the timescales of the bacterial incubation assays discussed below.

3.4. *S. epidermidis* Adhesion Modulated Chiefly by Substrata Mechanical Compliance. We leveraged the above ensemble of substrata in a 2 h incubation of 10^7 cells/mL in deionized water and observed the average colony density following 24 h culture under 1% agar. *S. epidermidis* remained viable in ion-free suspensions that were well in excess of the duration of the attachment assays. Figure 3a demonstrates strong positive correlation between the substrata elastic moduli and colony density, with an approximately 100-fold increase in colony density for a 100-fold increase in substrata stiffness. As substrata stiffness may be correlative with physicochemical surface interactions that more strongly or more directly affect this initial bacterial adhesion, we also considered correlations with surface roughness, total interaction energy, and charge density. The rms surface roughness varied among the substrata from 3 to 30 nm, yet Figure 3b indicates no discernible effect on bacterial attachment over this range and distribution of surface roughness. Figure 3c shows that the surface interaction energy of the *S. epidermidis*−water−PEM system ΔG_{MWP} was statistically indistinguishable (1-way ANOVA, $a = 0.05$, $P = 0.987$) among these mechanically dissimilar substrata. Finally, we found net surface charge density to be quite similar for the two substrata that differed most in both surface roughness and mechanical compliance (PEMs assembled at pH 2.0 and 6.5). In fact, Figure 3d shows that the slight interfacial electrostatic repulsion of these PEMs in deionized water (~ -3 mC/m^2) extends less than 20 nm from the PEM surface. This interaction distance is small compared to the projected length of bacteria fimbriae or pili that extend 500 to 1000 nm from the bacterial cell surface,[22,50,51] suggesting one mechanism by which bacteria overcome such electrostatic repulsion. Thus, at least for substrata of comparable surface interaction energies and charge density, it appears that adhesion of viable *S. epidermidis* can be modulated by the mechanical stiffness of the substrata. For the physicochemical properties quantified here, *S. epidermidis* colony density increases with increasing substrata stiffness over the range of 1 MPa $< E <$ 100 MPa.

To further test this hypothesis, we employed the tunability of layer-by-layer assembly to gradually alter effective compliance of the PEM surface. After assembling stiff substrata at pH 6.5, we then added 0.5 and 1 bilayer of the compliant PEM at pH 2.0; after assembling compliant substrata at pH 2.0, we added 0.5 bilayer of the stiff PEM at pH 6.5 (see Experimental Section). As expected, E of the stiff PEM surface decreased upon addition of compliant layers from the extrema of $E \sim 100$ MPa (pH 6.5) to ~ 30 MPa (pH 2.0, 0.5 bilayer) and ~ 1 MPa (pH 2.0, 1 bilayer). Effective E of the compliant PEM increased to $E \sim 100$ MPa when topped with PAH 6.5, due ostensibly to polycation interpenetration and crosslinking.[52] Figure 4 demonstrates that by changing the effective substrata compliance through this approach, *S. epidermidis* colony density progressively decreased with increasing PEM compliance. The assembly of such composite films has the potential to alter other surface characteristics within this substrata set, but the strong correlation between effective substrata stiffness and colony density is retained. This gradual masking of mechanoselective adhesion is consistent with previous studies on eukaryotic cells[32] but is observed here after addition of just a single compliant polyelectrolyte layer; decreased adhesion of fibroblasts is not observed until addition of at least five bilayers of the compliant PEM to the stiff PEM. This may be attributed in part to the increased forces and distances over which eukaryotic cells can strain the underlying substrata through actomyosin traction at focal adhesions of diameters comparable to a single bacterium.[53,54]

3.5. Mechanoselective Adhesion is Independent of Monovalent Ion Concentration. To consider whether the presence of the monovalent ions in 150 mM NaCl phosphate-buffered saline (PBS) strongly affected the observed trends, bacterial attachment to the most mechanically distinct PEMs (assembled at pH 2.0 and 6.5) was monitored over a titration of salt concentrations. Solution molarity of 150 mM approximates physiological ionic strength, and the absence of Ca^{2+} and Mg^{2+} ions approximates low extracellular calcium levels predominantly complexed with serum albumin or negative ions.[55] Figure 5 shows that there is no major change in colony density with increased solution ionic strength (pure water to 150 mM NaCl PBS). More generally, this suggests that the molecular agents involved in this mechanosensation are not sensitive to monovalent ionic strength changes over this broad spectrum. Additionally, the Debye screening length, the distance from the substrata surface over which electrostatic effects extend through the aqueous media, is a function of the ionic strength and is $\sim$100 nm in water (Figure 3d) and $<$1 nm at the highest ionic strength assayed.[28] One may reasonably conclude that the effect of surface charge density and its associated free energy on bacterial adhesion are negligible under all solution molarities in this system, because there is no significant change in the adhesion response as the screening length is modulated across different length scales. This titration result is particularly interesting in light of recent hypotheses that bacterial sensing of mechanical stimuli may occur through stretch-induced activation of transient receptor potential (TRP) ion channels.[56–58] Our results suggest that activation of mechanosensitive TRP ion channels is not required. It is also now known that some bacteria possess analogs to eukaryotic mechanoactive cytoskeletal components, including actin analogues such as *mreB*, molecular motors, and integrin analogues.[59] However, although *S. epidermidis* have been shown to express ftsZ (a tubulin analogue that is chiefly

Table 1. PEMs Used To Test Physicochemical and Mechanical Properties Affecting Bacterial Attachment

assembly pH[a](PAA/PAH)	symbol[b]	ΔG_{MWP} (mJ/m^2)[c,d]	rms roughness (nm)[d,e]	E (MPa)[d,f]
2.0/2.0	▼	29.0 ± 7.5	30.2 ± 29.5	0.75 ± 0.05
6.5/6.5	●	27.2 ± 9.0	2.7 ± 1.6	80.4 ± 38.0
3.5/7.5	■	27.2 ± 8.0	12.2 ± 9.0	36.6 ± 5.7
3.5/8.6	♦	27.0 ± 6.9	18.5 ± 16.6	73.2 ± 16.6

[a] Assembly pH of polyanion and polycation indicated, respectively, for PEMs assembled to ~50 nm dry thickness (≥57 nm hydrated thickness) with PAA as the last layer. [b] Symbols used throughout to indicate the corresponding PEM in all figures. [c] Total interaction energy ΔG_{MWP} of the microbe−water−polymer system. [d] All data expressed as average ± standard deviation. [e] Root mean square (rms) surface roughness. [f] Nominal elastic moduli E.

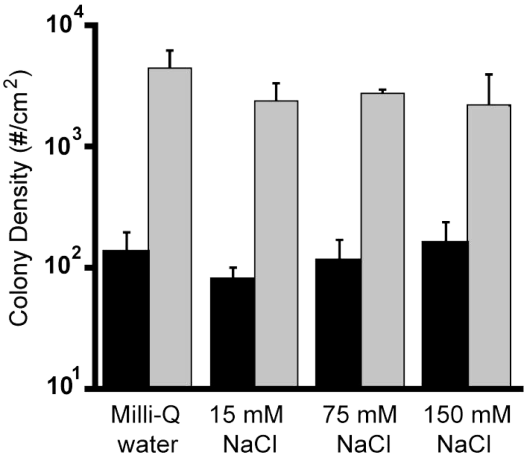

Figure 5. *S. epidermidis* colony density as a function of solution ion concentration. Colony density on compliant substrata (black, $E \sim 1$ MPa) is lower than that on stiff substrata (gray, $E \sim 100$ MPa), regardless of solution monovalent ion concentration in which 10^7 cells/mL were incubated with substrata. This suggests that activation of mechanosensitive monovalent ion channels is not required of mechanoselective adhesion in these bacteria.

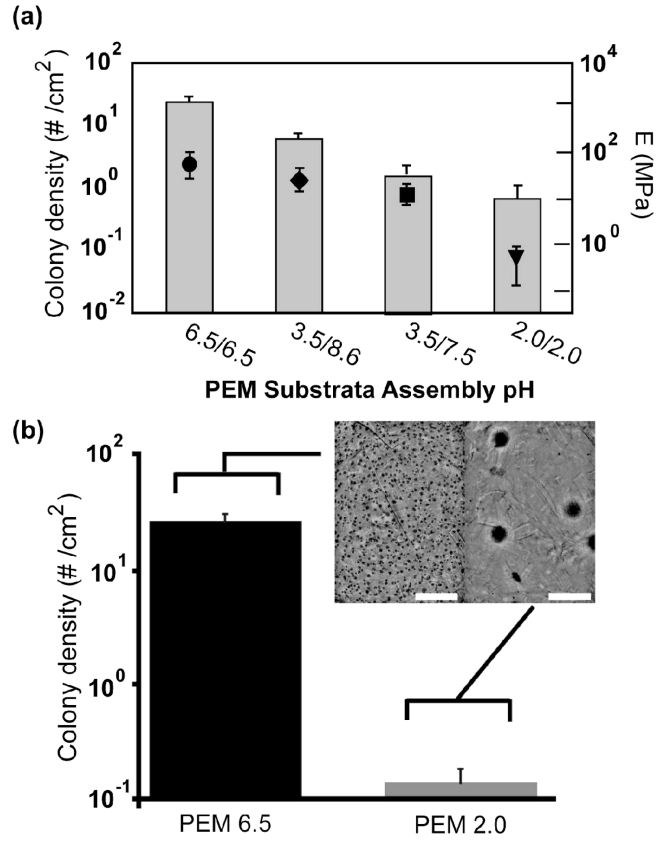

Figure 6. (a) Wild-type *E. coli* exhibit colony density (bars) that varies directly with the stiffness (symbols) of the PEM substrata. (b) Viable, spherical Δ*mreB E. coli* that lack the actin analogue *mreB* also adhere more readily to the stiffest substrata ($E \sim 100$ MPa) than to the most compliant substrata ($E \sim 1$ MPa). Scalebars = 1 mm.

involved in cell division), these bacteria have not been shown to express actin analogues presumed to be required of eukaryotic mechanotransduction via macromolecular focal contacts with the substratum material.[56]

3.6. Mechanoselective Adhesion is also Exhibited by Wild-Type and Mutant *E. coli*. The above results raise the possibility that mechanoselective adhesion may be unique to this particular strain of *S. epidermidis*. To address this issue and further probe the origins of this mechanoselectivity, we also used the same suite of PEM substrata to assay the adhesion efficiency of wild-type (wt) *E. coli* (K-12 w3100 strain) and a spherical mutant form, Δ*mreB*. This mutant lacks the *mreBCD* operon responsible for the actin analogue *mreB* and, thus, the rod-like shape of *E. coli*. Additionally, *E. coli* are G−, whereas *S. epidermidis* are G+, indicating structural differences in the bacterial cell envelope. As wt *E. coli* adhesion efficiency to control surfaces (e.g., to glass) exceeded that of *S. epidermidis* under these incubation conditions, the *E. coli* seeding density in these experiments was reduced to 0.5×10^7 cells/mL; otherwise, all experimental conditions were identical to those used in the *S. epidermidis* experiments reported in Figure 3. Figure 6a shows that the colony density of wt *E. coli* increases directly with increasing PEM substrata stiffness over the previously detailed range of 1 MPa < E < 100 MPa. This represents approximately a 1000-fold decrease in colony density over a 100-fold reduction in E; on a proportional basis, this is a larger reduction in adhesion efficiency than observed for the *S. epidermidis*. Thus, despite the differences between the biochemical compositions of spherical *S. epidermidis* and rod-like *E. coli*, both cell types exhibit mechanoselective adhesion over this range of substrata stiffness. As in the case of *S. epidermidis* cultured with the same defined substrata, there was no correlation between colony density and substrata characteristics, including surface roughness, total interaction energy, or charge density. We note that the relatively greater cell surface area of *E. coli* (2−8-fold)[60,61] may contribute to the enhanced adhesion efficiencies of this bacterium to these surfaces; further studies are required to explore this possibility.

To consider the effects of cell shape conferred by protein expression, without the concomitant effects of varied extracellular envelope composition, we also assayed the adhesion efficiency of spherical Δ*mreB E. coli* to the substrata of extreme mechanical compliance. Figure 6b demonstrates that the colony density of this actin analogue-mutated, G− microbe also correlated directly with PEM substrata stiffness. These Δ*mreB E. coli* exhibited a 100-fold reduction in colony density with a 100-fold decrease in E, a rate of change comparable to that observed for the spherical *S. epidermidis* over the same range of conditions. Thus, although this represents an admittedly incomplete survey of bacterial strains and types, these data demonstrate that the correlation of viable bacteria adhesion

efficiency with substrata stiffness is not unique to only the G+, spherical *S. epidermidis*. Bakker et al. have noted mild, positive correlation of substrata stiffness with adhesion of marine bacterial strains under certain flow chamber conditions, but not others, to polyurethane surfaces;[62,63] these authors considered much stiffer substrata over a considerably narrower range of E than those of the present study (1500 MPa $< E <$ 1900 MPa) and did not report possible differences in surface charge density among those substrata. Thus, systematic consideration of the generality of this dependence for other bacterial strains, incubation conditions and substrata characteristics, including stiffness, remains an important topic for future studies.

Although complete elucidation of the molecular mechanisms responsible for this new observation is beyond the focus of this paper, our results indicate that neither stretch responsive monovalent ion channels, cell envelope composition indicated by Gram-staining, nor cell shape are required and/or causal elements. Alternatively, it is possible that bacterial fimbriae/pili, which are constitutively expressed by the bacteria considered herein,[22,50,51] mediate a mechanoselective process similar to the so-called catch-bond mechanism posited to explain effects of shear flow stress on cell adhesion dynamics: the lifetime of noncovalent interactions can be increased under external mechanical force.[56,64] As bacterial pili collide with and sample the substrata during incubation, the mechanical resistance of the material to pili retraction would increase with increasing substrata stiffness; this stabilization on stiffer substrata could increase the lifetime of pili-substrata interactions during the fast step of bacterial two-stage binding kinetics.[22] *S. epidermidis* and *E. coli* possess several glycosylated substructures at both the pili and the extracellular capsule[22,50,51] that are known to form attachments to materials and are capable of complex interactions similar to those observed in other bacterial species reported to form pili catch-bonds. Thorough consideration of this and other proposed mechanisms of this mechanoselective adhesion is the focus of ongoing work. Together, these results do not invalidate the physicochemical effects reported to influence microbial adhesion. Clearly, several competing surface features affect bacterial adhesion, viability, and subsequent colonization. Rather, the current study demonstrates that mechanical compliance of the substrata presents an important additional factor contributing to stable adhesion of viable bacteria.

4. Conclusions

We find that the adhesion of viable, colony-forming *S. epidermidis* and *E. coli* correlates positively with increasing elastic modulus of weak polyelectrolyte multilayered substrata over the range 1 MPa $< E <$ 100 MPa. To our knowledge, this is the first demonstration that substrata stiffness affects the adhesion of viable prokaryotes, such as bacteria, independently of other surface characteristics. These observations were not attributable to differences in posited physicochemical regulators of bacterial adhesion, including rms surface roughness, surface interaction energy, and surface charge density of the PEM thin films. For the bacteria concentrations considered, neither divalent ions nor monovalent ions such as Na^+ and Cl^- are required for this mechanosensory function, suggesting that activation of TRP ion channels is not required for mechanoselective adhesion of *S. epidermidis*. Further, quantitatively similar trends in wt and Δ*mreB E. coli* confirmed that this correlation is not limited to a single type or shape of bacteria. Although the underlying mechanisms require further study, it is clear that the mechanical stiffness of nanoscale polymeric substrata can strongly modulate adhesion of viable bacteria in aqueous suspensions, independently of several other interactions at the cell−material interface. Thus, mechanical compliance of material surfaces represents an additional design parameter by which colonization of both beneficial and potentially infectious bacteria can be modulated.

Acknowledgment. The authors acknowledge use of the MIT Department of Materials Science & Engineering Nanomechanical Technology Laboratory and assistance from K. Furman and Y. Kim (MIT). This work was supported in part by the MRSEC Program of the National Science Foundation under Award Number DMR-02-13282; NIH Bioinformatics Training Grant (M.T.T.); NSF Graduate Fellowship Program (J.A.L.); and NSF CAREER Award and the Arnold and Mabel Beckman Foundation Young Investigator Program (K.J.V.V.).

Supporting Information Available. Additional experimental procedures detailing mechanical analysis of PEMs, calculations of surface energy, interaction energy, and charge density, and colony image analysis. Additional table listing individual surface energy components for bacteria, substrata, and solvents. This material is available free of charge via the Internet at http://pubs.acs.org.

References and Notes

(1) Katsikogianni, M.; Missirlis, Y. F. *Eur. Cells Mater.* **2004**, *8*, 37–57.
(2) Klevens, R. M.; Edwards, J. R.; Richards, C. L.; Horan, T. C.; Gaynes, R. P.; Pollock, D. A.; Cardo, D. M. *Public Health Rep.* **2007**, *122*, 160–166.
(3) Donlan, R. M. *Emerging Infect. Dis.* **2001**, *7*, 277–81.
(4) Costerton, J. W.; Stewart, P. S.; Greenberg, E. P. *Science* **1999**, *284*, 1318–22.
(5) Chang, C. C.; Merritt, K. *J. Biomed. Mater. Res.* **1992**, *26*, 197–207.
(6) Tiller, J. C.; Lee, S. B.; Lewis, K.; Klibanov, A. M. *Biotechnol. Bioeng.* **2002**, *79*, 465–71.
(7) Tiller, J. C.; Liao, C. J.; Lewis, K.; Klibanov, A. M. *Proc. Natl. Acad. Sci. U.S.A.* **2001**, *98*, 5981–5.
(8) Lee, D.; Cohen, R. E.; Rubner, M. F. *Langmuir* **2005**, *21*, 9651–9659.
(9) Li, Z.; Lee, D.; Sheng, X. X.; Cohen, R. E.; Rubner, M. F. *Langmuir* **2006**, *22*, 9820–9823.
(10) Saygun, O.; Agalar, C.; Aydinuraz, K.; Agalar, F.; Daphan, C.; Saygun, M.; Ceken, S.; Akkus, A.; Denkbas, E. B. *J. Surg. Res.* **2006**, *131*, 73–9.
(11) Hetrick, E. M.; Schoenfisch, M. H. *Chem. Soc. Rev.* **2006**, *35*, 780–789.
(12) Kohnen, W.; Kolbenschlag, C.; Teske-Keiser, S.; Jansen, B. *Biomaterials* **2003**, *24*, 4865–9.
(13) Ignatova, M.; Voccia, S.; Gilbert, B.; Markova, N.; Cossement, D.; Gouttebaron, R.; Jerome, R.; Jerome, C. *Langmuir* **2006**, *22*, 255–62.
(14) Etienne, O.; Picart, C.; Taddei, C.; Haikel, Y.; Dimarcq, J. L.; Schaaf, P.; Voegel, J. C.; Ogier, J. A.; Egles, C. *Antimicrob. Agents and Chemother.* **2004**, *48*, 3662–3669.
(15) Rudra, J. S.; Dave, K.; Haynie, D. T. *J. Biomater. Sci., Polym. Ed.* **2006**, *17*, 1301–1315.
(16) Boulmedais, F.; Frisch, B.; Etienne, O.; Lavalle, P.; Picart, C.; Ogier, J.; Voegel, J. C.; Schaaf, P.; Egles, C. *Biomaterials* **2004**, *25*, 2003–2011.
(17) Teixeira, P.; Trindade, A. C.; Godinho, M. H.; Azeredo, J.; Oliveira, R.; Fonseca, J. G. *J. Biomater. Sci., Polym. Ed.* **2006**, *17*, 239–46.
(18) Cao, T.; Tang, H.; Liang, X.; Wang, A.; Auner, G. W.; Salley, S. O.; Ng, K. Y. *Biotechnol. Bioeng.* **2006**, *94*, 167–76.
(19) Tang, H.; Cao, T.; Wang, A.; Liang, X.; Salley, S. O.; McAllister, J. P. 2nd;.; Ng, K. Y. *J. Biomed. Mater. Res. A* **2007**, *80*, 885–94.
(20) Katsikogianni, M.; Spiliopoulou, I.; Dowling, D. P.; Missirlis, Y. F. *J. Mater. Sci.: Mater. Med.* **2006**, *17*, 679–89.
(21) An, Y. H.; Friedman, R. J. *J. Biomed. Mater. Res.* **1998**, *43*, 338–348.
(22) Ofek, I.; Hasty, D. L.; Doyle, R. J. *Bacterial Adhesion to Animal Cells and Tissues*; American Society for Microbiology: Washington DC, 2003.
(23) Ilker, M. F.; Nusslein, K.; Tew, G. N.; Coughlin, E. B. *J. Am. Chem. Soc.* **2004**, *126*, 15870–5.

(24) MacKintosh, E. E.; Patel, J. D.; Marchant, R. E.; Anderson, J. M. *J. Biomed. Mater. Res. A* **2006**, *78*, 836–42.
(25) Triandafillu, K.; Balazs, D. J.; Aronsson, B. O.; Descouts, P.; Tu Quoc, P.; van Delden, C.; Mathieu, H. J.; Harms, H. *Biomaterials* **2003**, *24*, 1507–18.
(26) Abu-Lail, N. I.; Camesano, T. A. *Langmuir* **2006**, *22*, 7296–301.
(27) Speranza, G.; Gotterdi, G.; Pederzolli, C.; Lunelli, L.; Canteri, R.; Pasquardiini, L.; Carli, E.; Lui, A.; Maniglio, D.; Brugnara, M.; Anderle, M. *Biomaterials* **2004**, *25*, 2029–2037.
(28) van Oss, C. J. *J. Mol. Recognit.* **2003**, *16*, 177–190.
(29) Kang, S.; Choi, H. *Colloids Surf., B* **2005**, *46*, 70–77.
(30) Liu, Y.; Strauss, J.; Camesano, T. A. *Langmuir* **2007**, *23*, 7134–42.
(31) Richert, L.; Engler, A. J.; Discher, D. E.; Picart, C. *Biomacromolecules* **2004**, *5*, 1908–16.
(32) Mendelsohn, J. D.; Yang, S. Y.; Hiller, J.; Hochbaum, A. I.; Rubner, M. F. *Biomacromolecules* **2003**, *4*, 96–106.
(33) Thompson, M. T.; Berg, M. C.; Tobias, I. S.; Rubner, M. F.; Van Vliet, K. J. *Biomaterials* **2005**, *26*, 6836–6845.
(34) Discher, D. E.; Janmey, P.; Wang, Y. L. *Science* **2005**, *310*, 1139–1143.
(35) Schneider, A.; Francius, G.; Obeid, R.; Schwinte, P.; Hemmerle, J.; Frisch, B.; Schaaf, P.; Voegel, J. C.; Senger, B.; Picart, C. *Langmuir* **2006**, *22*, 1193–1200.
(36) Mack, D.; Rohde, H.; Harris, L. G.; Davies, A. P.; Horstkotte, M. A.; Knobloch, J. K. *Int. J. Artif. Organs* **2006**, *29*, 343–59.
(37) Danese, P. N. *Chem. Biol.* **2002**, *9*, 873–80.
(38) Arciola, C. R.; Campoccia, D.; Gamberini, S.; Donati, M. E.; Pirini, V.; Visai, L.; Speziale, P.; Montanaro, L. *Biomaterials* **2005**, *26*, 6530–6535.
(39) van der Kooij, D.; Veenendaal, H. R.; Scheffer, W. J. *Water Res.* **2005**, *39*, 2789–98.
(40) Janmey, P. A.; McCulloch, C. A. *Annu. Rev. Biomed. Eng.* **2007**, *9*, 1–34.
(41) Thompson, M.; Berg, M.; Tobias, I.; Lichter, J.; Rubner, M.; Van Vliet, K. *Biomacromolecules* **2006**, *7*, 1990–1995.
(42) Shiratori, S. S.; Rubner, M. F. *Macromolecules* **2000**, *33*, 4213–4219.
(43) Richert, L.; Lavalle, P.; Vautier, D.; Senger, B.; Stoltz, J.-F.; Schaaf, P.; Voegel, J. C.; Picart, C. *Biomacromolecules* **2002**, *3*, 1170–1178.
(44) Hutter, J.; Bechhoefer, J. *Rev. Sci. Instrum.* **1993**, *64*, 1868–1873.
(45) Dean, D.; Han, L.; Grodzinsky, A. J.; Ortiz, C. *J. Biomech. Eng.* **2006**, *39*, 2555–65.
(46) Rixman, M.; Dean, D.; Macais, C.; Ortiz, C. *Langmuir* **2003**, *19*, 6202–6218.
(47) Bachmann, B. J. *Bacteriol. Rev.* **1972**, *36*, 525–557.
(48) Arnsdorf, M. F.; Knight, B. P. Patient Information: Implantable cardiodefibrillators. *UpToDate*, 2006.
(49) Kostler, S.; Delgado, A. V.; Ribitsch, V. *J. Colloid Interface Sci.* **2005**, *286*, 339–348.
(50) Banner, M. A.; Cunniffe, J. G.; Macintosh, R. L.; Foster, T. J.; Rohde, H.; Mack, D.; Hoyes, E.; Derrick, J.; Upton, M.; Handley, P. S. *J. Bacteriol.* **2007**, *189*, 2793–804.
(51) Veenstra, G. J.; Cremers, F. F.; van Dijk, H.; Fleer, A. *J. Bacteriol.* **1996**, *178*, 537–41.
(52) Francius, G.; Hemmerle, J.; Ball, V.; Lavalle, P.; Picart, C.; Voegel, J. C.; Schaaf, P.; Senger, B. *J. Phys. Chem. C* **2007**, *111*, 8299–8306.
(53) Oommen, B.; Van Vliet, K. J. *Thin Solid Films* **2006**, *25*, 235–242.
(54) Walton, E. B.; Oommen, B.; Van Vliet, K. J. In *Engineering in Medicine and Biology*; Layton, B., Ed.; Lyon, France, 2007.
(55) Greenspan, F. S.; Gardner, D. G. *Basic and Clinical Endocrinology*, 7th ed.; Lange Medical Books/McGraw-Hill Publishing: New York, 2004.
(56) Vogel, V. *Annu. Rev. Biophys. Biomol. Struct.* **2006**, *35*, 459–88.
(57) Anishkin, A.; Kung, C. *Curr. Opin. Neurobiol.* **2005**, *15*, 397–405.
(58) Lin, S. Y.; Corey, D. P. *Curr. Opin. Neurobiol.* **2005**, *15*, 350–7.
(59) Shih, Y. L.; Rothfield, L. *Microbiol. Mol. Biol. Rev.* **2006**, *70*, 729–754.
(60) Koch, A. L.; Woeste, S. *J. Bacteriol.* **1992**, *174*, 4811–4819.
(61) Sundararaj, S.; Guo, A.; Habibi-Nazhad, B.; Rouani, M.; Stothard, P.; Ellison, M.; Wishart, D. S. *Nucleic Acids Res.* **2004**, *32*, D293–D295.
(62) Bakker, D. P.; Busscher, H. J.; van Zanten, J.; de Vries, J.; Klijnstra, J. W.; van der Mei, H. C. *Microbiology* **2004**, *150*, 1779–1784.
(63) Bakker, D. P.; Huijs, F. M.; de Vries, J.; Klijnstra, J. W.; Busscher, H. J.; van der Mei, H. C. *Colloids Surf., B* **2003**, *32*, 179–190.
(64) Thomas, W.; Forero, M.; Yakovenko, O.; Nilsson, L.; Vicini, P.; Sokurenko, E.; Vogel, V. *Biophys. J.* **2006**, *90*, 753–64.

BM701430Y

2008, Volume 9

Jenny A. Lichter, M. Todd Thompson, Maricela Delgadillo, Takehiro Nishikawa, Michael F. Rubner, and Krystyn J. Van Vliet*: Substrata Mechanical Stiffness Can Regulate Adhesion of Viable Bacteria

Pages 1574 and 1576. The caption of Figure 3 and the second column of Table 1 both contain an inadvertent switch of the symbols used to distinguish PEM 3.5/7.5 and 3.5/8.6 in the figures. In both the caption of Figure 3 and Table 1, 3.5/7.5 should be indicated as the filled diamond and 3.5/8.6 should be indicated as the filled square. The graphs within Figure 3 and the data within Table 1 remain unchanged.

Page 1575. The rightmost vertical axis of Figure 4 includes a typographical error on the log scale. The placement of 10^0 and 10^{-1} should be reversed, as $10^{-1} < 10^0$. The data were graphed correctly, and only the vertical axis was mislabeled at these positions.

BM8009335

10.1021/bm8009335

Published on Web 08/28/2008